

AXL receptor is required for Zika virus strain MR-766 infection in human glioblastoma cell lines

Samuel D. Zwernik,¹ Beau H. Adams,¹ Daniel A. Raymond,¹ Catherine M. Warner,¹ Amin B. Kassam,² Richard A. Rovin,² and Parvez Akhtar¹

¹Advocate Aurora Research Institute, Advocate Aurora Health, Milwaukee, WI 53233, USA; ²Aurora Neuroscience Innovation Institute, Advocate Aurora Health, Milwaukee, WI 53215, USA

Recent reports have shown that Zika virus (ZIKV) has oncolytic potential against human glioblastoma (GBM); however, the mechanisms underlying its tropism and cell entry are not completely understood. The receptor tyrosine kinase AXL has been identified as an entry receptor for ZIKV in a cell-type-specific manner. Interestingly, AXL is frequently overexpressed in GBM patients. Using commercially available GBM cell lines, we first show that cells expressing AXL are permissive for ZIKV infection, while cells that do not express AXL are not. Furthermore, inhibition of AXL kinase using R428 and antibody blockade of AXL receptor strongly attenuated virus entry in GBM cell lines. Additionally, CRISPR knockout of the AXL gene in GBM cell lines completely abolished ZIKV infection, significantly inhibited viral replication, and significantly reduced apoptosis compared with parental lines. Lastly, introduction of AXL receptor into non-expressing cell lines renders the cells susceptible to ZIKV infection. Together, these findings demonstrate that ZIKV entry into GBM cells *in vitro* is mediated by the AXL receptor and that following cell entry, productive infection is cytotoxic. Thus, ZIKV is a potential oncolytic virus for GBM.

INTRODUCTION

The median survival for patients with glioblastoma (GBM) is 15 months with the current standard of care treatment.¹ This standard has not changed since it was first approved in 2005, nor has the median survival for patients with GBM.² As treatments have not evolved and survival has not improved, novel treatment strategies such as oncolytic viruses merit consideration. Oncolytic viruses are defined as native or genetically modified viruses that can selectively kill tumor cells while sparing the healthy ones.^{3,4}

Zika virus (ZIKV) is an enveloped single-stranded RNA virus in the Flaviviridae family. The outbreak of ZIKV-induced fetal microcephaly and congenital Zika syndrome has spurred extensive research into its cell tropism.^{5–7} ZIKV shows remarkable tropism for fetal neural stem cells, entering them through the tyro-

sine kinase receptor AXL with resultant cytotoxicity.^{8–10} AXL is a member of the TAM family of tyrosine kinase receptors. AXL signaling impacts multiple cellular pathways and functions including survival, migration, proliferation, invasion, and immune suppression.^{11–13} Recent reports have identified AXL as a potential entry receptor for ZIKV in human glial cells, astrocytes, endothelial cells, skin cells, and Sertoli cells.^{14–19} However, data on the role of AXL in ZIKV entry is conflicting and appears to be cell type specific.^{15,20–22} For example, TAM receptors are not required for ZIKV entry and infection in mouse *in vivo* studies.^{23,24}

Interestingly, AXL is overexpressed in human glioblastoma.²⁵ Recent studies reported that ZIKV selectively kills human glioblastoma cancer stem cells and could have therapeutic potential for patients with GBM.^{26–29} However, it is not known whether ZIKV tropism for GBM occurs through the AXL receptor. One recent study showed that ZIKV targets glioblastoma cancer stem cells through a sox2-integrin $\alpha_V\beta_5$ axis.³⁰ In the present study, we sought to determine whether AXL-mediated entry is necessary and sufficient for ZIKV infection in commercially available human glioblastoma cell lines. The results of this study will help determine the suitability of ZIKV as an oncolytic virus.

RESULTS

ZIKV infects AXL-expressing glioblastoma cells

To evaluate the role of AXL in ZIKV infection of GBM cells, we first documented AXL protein levels in GBM cells by immunoblot. LN-229, U-87 MG, U-251 MG, and A-172 GBM cells demonstrated substantially higher levels of AXL protein (Figure 1A) compared with MDA-468 breast cancer cells.

Received 18 June 2021; accepted 8 November 2021;
<https://doi.org/10.1016/j.omto.2021.11.001>.

Correspondence: Parvez Akhtar, Advocate Aurora Research Institute, Advocate Aurora Health, Milwaukee, WI 53233, USA.

E-mail: parvez.akhtar@aah.org

Correspondence: Richard A. Rovin, Aurora Neuroscience Innovation Institute, Advocate Aurora Health, Milwaukee, WI 53215, USA.

E-mail: richard.rovin@aah.org



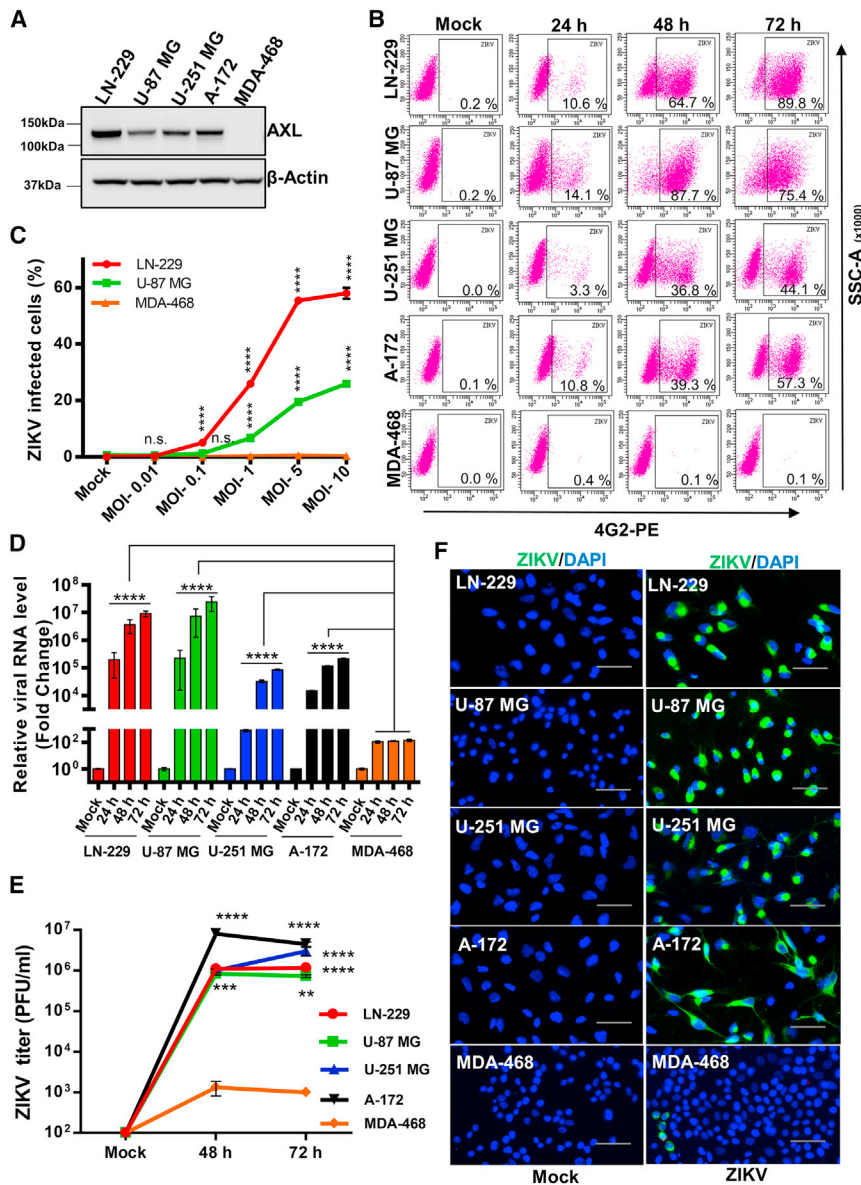


Figure 1. AXL-expressing cell lines are permissive to ZIKV (strain MR-766) infection

(A) Relative protein expression level of AXL in human glioblastoma (LN-229, U-87 MG, U-251 MG, and A-172) and breast cancer (MDA-468) cell lines. (B) The human glioblastoma and breast cancer cell lines were challenged with ZIKV at MOI 1. At 24, 48, and 72 hpi, the percentage of infected cells were quantified by flow cytometry. (C) AXL-expressing glioblastoma (LN-229 and U-87 MG) and AXL-negative breast cancer (MDA-468) cell lines were infected with increasing MOI (0.01, 0.1, 1, 5, and 10) for 24 h, and the percentage of infected cells were quantified by flow cytometry. (D) Cell lines were challenged with ZIKV at MOI 1 for 24, 48, and 72 h. The relative expression of ZIKV NS3 RNA was quantified by qRT-PCR at each time point. (E) ZIKV titer (PFU/mL) comparison between cell lines in supernatants by plaque assay at 48 and 72 hpi infected at MOI 1. (F) Immunofluorescence staining for ZIKV in glioblastoma and breast cancer cell lines at 72 hpi at MOI 10. Images were acquired through an Olympus IX83 microscope. ZIKV, green; DAPI, blue. Scale bars, 50 μ m. In (C), (D), and (E) data shown are means \pm SD of averages of two biological replicates performed in triplicate. Significance was calculated using two-way ANOVA (n.s., not significant; ** p < 0.01, *** p < 0.001, **** p < 0.0001).

at MOI 0.01, 0.1, 1, 5, and 10 PFU/cell and evaluated by flow cytometry at 24 hpi. Even at MOI of 10, MDA-468 cells were resistant to ZIKV infection (Figure 1C).

Intracellular viral RNA was quantified by quantitative real-time PCR (qRT-PCR) at 24, 48, and 72 hpi at MOI of 1 PFU/cell. ZIKV RNA was detected in GBM cells challenged with the virus but not in mock-infected cells, as shown in Figure 1D. The number of viral transcripts were markedly higher in AXL-expressing GBM cells compared with AXL-negative MDA-468 cells. ZIKV titers were also measured in the cell supernatants by plaque assay at 48 and 72 hpi at MOI of 1 PFU/cell. The number of viral particles produced by each GBM cell line was similar and significantly higher compared with MDA-468 cells, as shown in the growth curve (Figure 1E).

The presence of intracellular ZIKV envelope protein was also evaluated by immunofluorescence assay (IFA). At 72 hpi at MOI of 10, no staining was observed in mock-infected cells. IFA confirmed robust ZIKV infection of GBM AXL-expressing cells but not the AXL-negative MDA-468 cells (Figure 1F). Taken together, these data show that AXL-expressing cells are permissive to ZIKV infection, with the magnitude of infection varying between cell lines. By contrast, AXL-negative cells are resistant to infection.

To compare the permissiveness of AXL-expressing GBM and AXL-negative breast cancer cells to infection, we challenged these cells with the ZIKV at multiplicity of infection (MOI) of 1 plaque-forming unit (PFU)/cell. The percentage of infected cells was quantified at 24, 48, and 72 h post infection (hpi) by flow cytometry using the flavivirus envelope monoclonal antibody 4G2. LN-229, U-87 MG, U-251 MG, and A-172 AXL-expressing GBM cells were productively infected by ZIKV to a varying degree, whereas AXL-negative MDA-468 cells were resistant to ZIKV infection (Figure 1B). Quantification of the level of AXL expression in the GBM cell lines from immunoblotting demonstrated a correlation with ZIKV entry (Figures S1A and S1B), whereas the more AXL was present in a cell line, the higher was the infection level observed. Cells were also infected

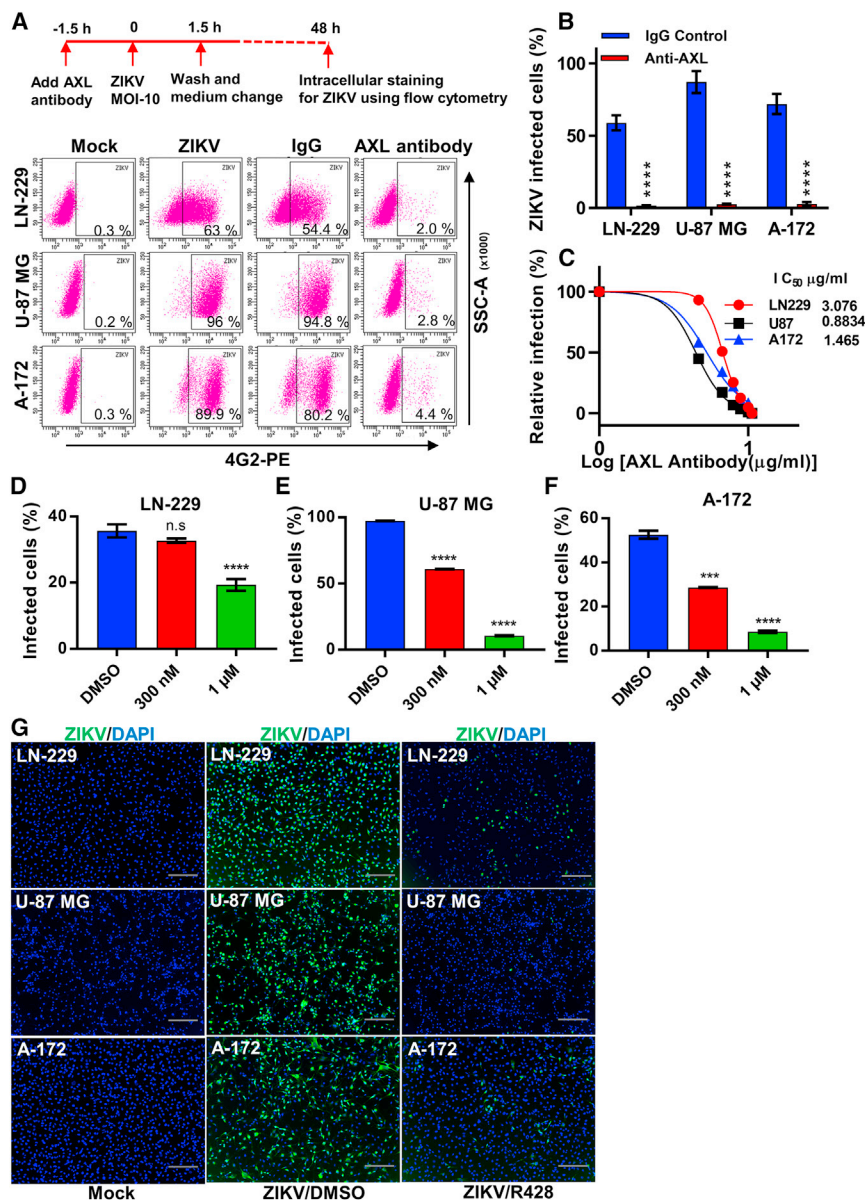


Figure 2. AXL is required for ZIKV infection of human glioblastoma cell lines

(A and B) Timeline of antibody blockade; cells were preincubated with a polyclonal anti-human AXL antibody for 90 min followed by ZIKV exposure (MOI 10) for 90 min, after which a wash and medium change was carried out (A), and the percentage of infected cells was quantified by flow cytometry 48 hpi (B). (C) Dose-response curve showing a decrease in cells infected with ZIKV as AXL antibody concentration is increased. (D–F) Human glioblastoma cells (LN-229 [D], U-87 MG [E], and A-172 [F]) were pretreated with R428 at indicated concentrations for 90 min followed by ZIKV infection (MOI 10) for 90 min, after which a wash and a medium change was carried out, and the percentage of infected cells was quantified by flow cytometry after 32 hpi. (G) LN-229, U-87 MG, and A-172 cells were pretreated with R428 with 1 μ M concentration or vehicle for 90 min; cells were then infected with ZIKV at MOI 10, with immunofluorescence staining of ZIKV at 32 hpi. ZIKV, green; DAPI, blue. Scale bars, 100 μ m. In (B), (D), (E), and (F), data shown are means \pm SD of averages of two biological replicates performed in triplicate. Significance was calculated using one-way ANOVA (n.s., not significant; *** p < 0.001, **** p < 0.0001).

Pretreatment of the GBM cell lines with R428, a selective small-molecule inhibitor of AXL kinase, prior to ZIKV exposure reduced infection. We found that the percentage of infected cells decreased in a dose-dependent manner (Figures 2D–2F). A 1 μ M concentration of R428 reduced ZIKV infection in LN-229 cells by approximately 40% (Figure 2C). The percentage of ZIKV-infected cells was reduced by more than 80% at 1 μ M R428 in U-87 MG and A-172 cells (Figures 2E and 2F). This significant reduction of ZIKV infection in R428 (1 μ M)-treated GBM cells was also confirmed by IFA at 32 hpi (Figure 2G).

To determine whether downstream AXL kinase activity is also required for ZIKV replication, we first infected LN-229 and U-87 MG cells with ZIKV at MOI of 1 PFU/cell and then treated them with R428 for 24 h. We found a significant decrease (80%–95%) in ZIKV replication at 1 μ M concentration (Figures 3A and 3B). R428 treatment did not have an independent cytotoxic effect on GBM cells after 32 h of exposure (Figure 3C). Taken together, these results indicate that the AXL receptor and downstream AXL kinase activity are required for ZIKV entry and infection of human GBM cells.

AXL CRISPR knockout in glioblastoma cells prevents ZIKV entry
To further demonstrate the role of the AXL receptor in ZIKV entry, we used a CRISPR construct to knock out AXL in LN-229 and U-251 MG glioblastoma cell lines and validated this by immunoblot (Figures 4A and 4B). There was no evidence of ZIKV infection in LN-229

AXL receptor blockade and inhibition significantly inhibits ZIKV entry in glioblastoma cells

To determine whether AXL expression is necessary for ZIKV entry, we preincubated AXL-positive GBM cells (LN-229, U-87 MG, and A-172) with an anti-AXL antibody to block the receptor binding site. At 48 hpi at MOI of 10 PFU/cell, antibody blockade of the AXL receptor reduced the number of ZIKV-infected cells by 95% compared with mock blockade or immunoglobulin G (IgG) blockade (Figures 2A and 2B). We next generated dose-response neutralization curves and calculated the IC₅₀ values for antibody blockade of ZIKV infection in LN-229, U-87 MG, and A-172 cell lines. As antibody concentration increased, ZIKV infection decreased. Moreover, IC₅₀ increased as the level of AXL expression increased (Figure 2C).

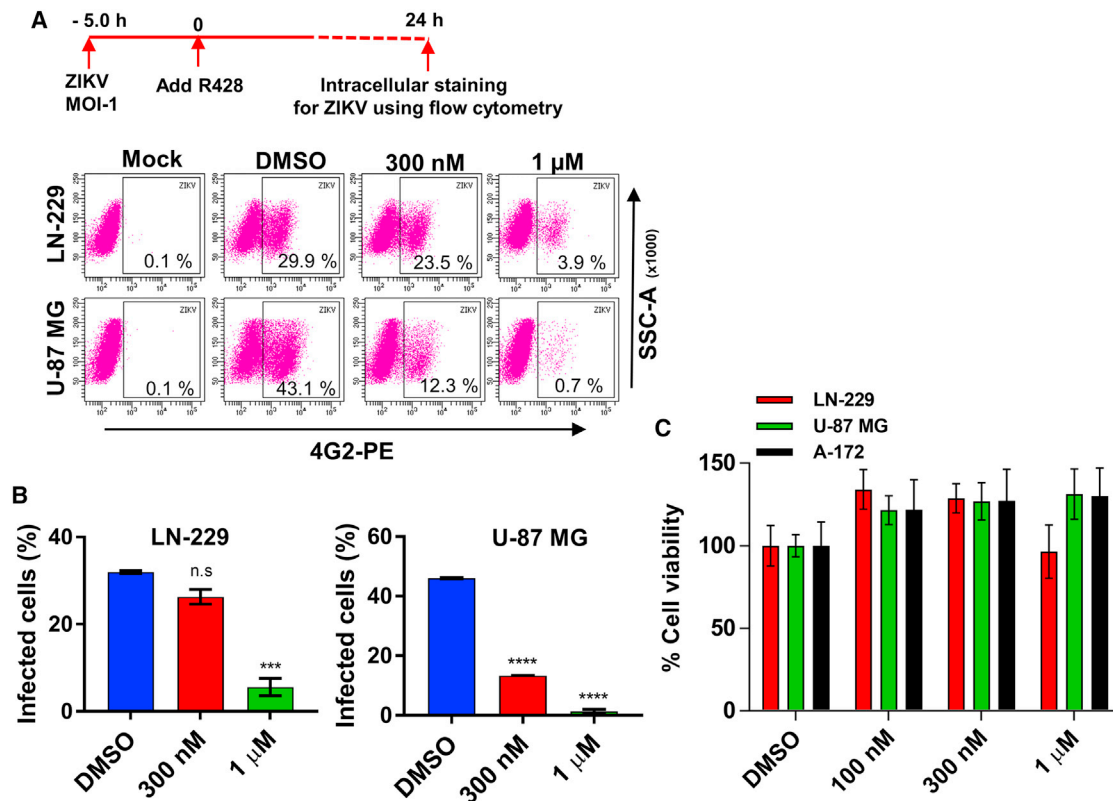


Figure 3. AXL kinase activity is required for ZIKV replication in human glioblastoma cell lines

(A and B) Timeline of post-exposure R428 treatment. LN-229 and U-87 MG cells were first infected at MOI 1 for 90 min. After 5 h the cells were treated with indicated concentrations of R428 or vehicle for 24 h (A). The percentage of infected cells were quantified by flow cytometry (B). (C) Cell viability was evaluated after R428 (0.1, 0.3, and 1 μM) or vehicle treatment in LN-229, U-87 MG, and A-172 glioblastoma cell lines. At 32 h, the WST-1 assay was used to determine cell viability. The percentage of viable cells was calculated after normalizing to the DMSO (vehicle) infected cells. In (B), data shown are means ± SD and are representative of three independent experiments. Significance was calculated using one-way ANOVA (n.s., not significant; ***p < 0.001, ****p < 0.0001).

AXL^{KO} cells (Figure 4C), nor was there evidence of intracellular viral RNA (Figure 4D). Similarly, no intracellular viral RNA was identified in U-251 MG AXL^{KO} cells following exposure to ZIKV at MOI 1 or 10 PFU/cell at 72 hpi. By contrast, viral RNA levels exponentially increased with increasing MOI in the parental U-251 MG cells (Figure 4E). ZIKV titers were also measured in the supernatants by plaque assay in parental and knockout cell lines at 48 and 72 hpi at MOI of 1 PFU/cell. The viral titers were markedly lower in the AXL^{KO} cell lines (Figure 4F). IFA showed a substantial reduction in intracellular ZIKV in LN-229 AXL^{KO} cells compared with the parental cell line at 72 hpi (Figure 4G). Similarly, CRISPR knockout of AXL in U-251 MG cells reduced intracellular ZIKV by more than 98% compared with the parental cell line 48 hpi at MOI 20 PFU/cell as determined by IFA (Figures 4H and 4I). Taken together, these results confirm that the AXL receptor is required for ZIKV entry and infection of commercially available GBM cell lines.

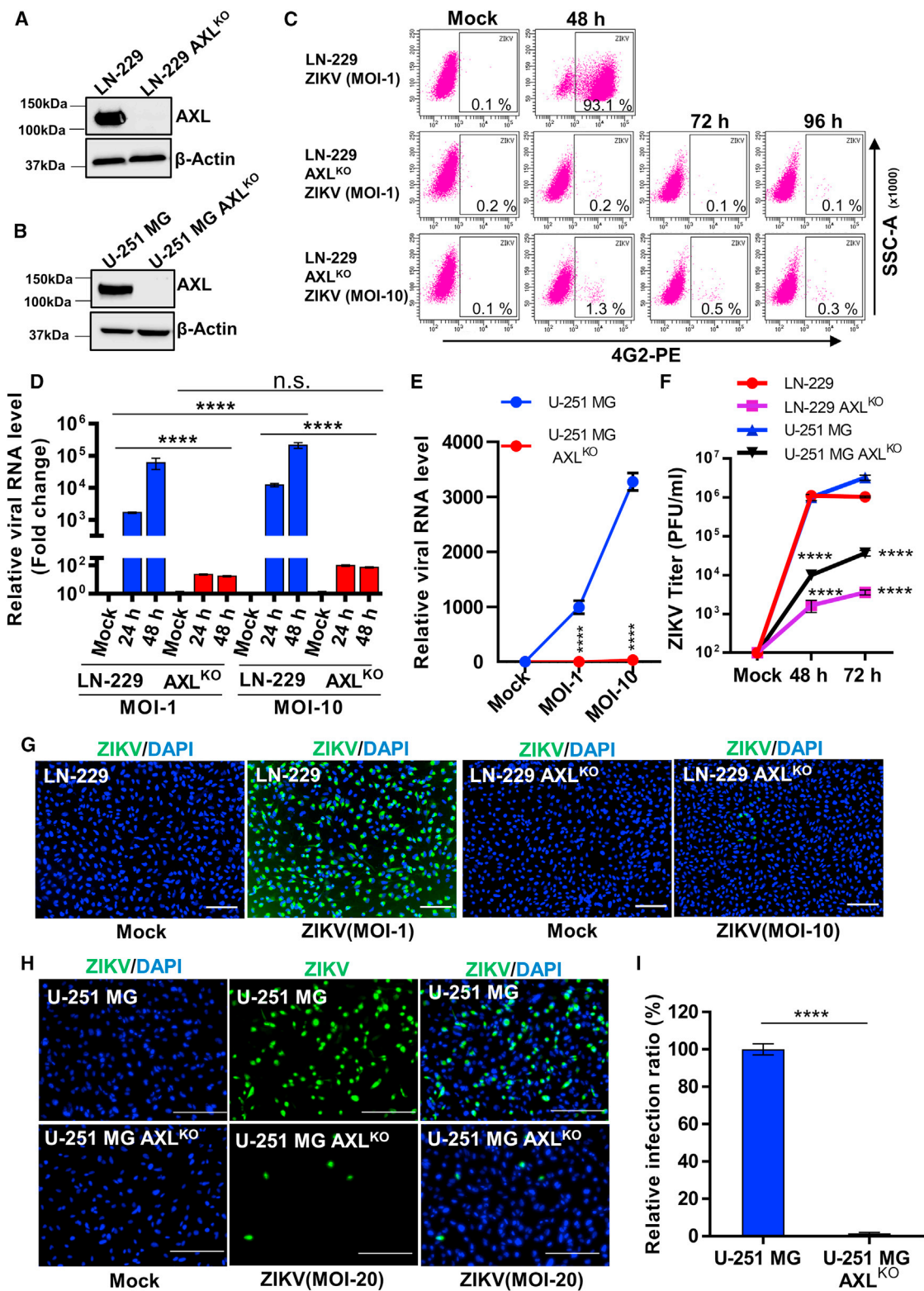
ZIKV induces apoptosis in AXL-expressing glioblastoma cells

Knowing that ZIKV can enter and replicate in AXL-expressing glioblastoma cell lines, we wanted to evaluate its cytopathic effects in LN-

229 and LN-229 AXL^{KO}. The effects of ZIKV on cell viability/death were first assessed using the cell proliferation reagent WST-1. We observed no significant cytopathic effects in the AXL^{KO} cells at any time point or MOI compared with the parental LN-229 cells (Figure 5A). Apoptosis was then evaluated with the Annexin V assay. ZIKV infection resulted in significant apoptosis in parental LN-229 cells but not in the AXL^{KO} cells (Figures 5B and 5C). These results indicate that ZIKV infection results in apoptotic cell death in AXL-expressing cell lines. In the absence of a functional AXL receptor, the CRISPR knockout cell lines are resistant to infection and subsequent cell death.

Functional AXL expression restores susceptibility to ZIKV infection

To further evaluate the significance of AXL receptor for ZIKV entry, we used an AXL lentivirus (pLenti-GIII-CMV-GFP-2A-Puro:AXL) construct to stably express AXL in MDA-468 and U-251 MG AXL^{KO} cell lines. AXL expression was validated by immunoblot (Figures 6A and 6D). MDA-468 and MDA-468::AXL cells were infected with ZIKV at MOI 20 PFU/cell. At 120 hpi, ZIKV entry was significantly



(legend on next page)

increased in MDA-468::AXL cells as shown by IFA (Figure 6B) and qRT-PCR for intracellular viral RNA (Figure 6C). Next, we infected U-251 MG AXL^{KO} and U-251 MG AXL^{KO}::AXL cell lines with ZIKV at MOI 20 PFU/cell for 24 and 48 h. At 48 hpi, intracellular ZIKV was markedly increased in U-251 MG AXL^{KO}::AXL cells compared with their parental knockout cell line (Figures 6E and 6F). The number of intracellular viral transcripts was markedly higher in AXL-expressing U-251 MG AXL^{KO}::AXL compared with U-251 MG AXL^{KO} cells, quantified by qRT-PCR (Figure 6G). Taken together, these results indicate that AXL receptor is required for ZIKV entry in GBM cell lines.

DISCUSSION

In this study we show that in commercially available human GBM cell lines ZIKV requires a functional AXL receptor for cell entry. We also show that once inside a GBM cell, ZIKV replication is robust and results in cytotoxicity. These characteristics, receptor-mediated entry and cytotoxicity, are two important hallmarks of an oncolytic virus.³¹ Therefore, ZIKV should be considered a potential oncolytic virus.

During his 1912 address to the Royal Society of Medicine as President of the Neurological Section, Dr. Howard Tooth documented the average survival of “gliomata” patients as 10.1 months.³² In 2005, Stupp et al. reported a median survival for patients with glioblastoma of 14.6 months using the current standard of care.² A century of surgical and diagnostic innovation, and a deeper understanding of the molecular and genetic pathogenesis of GBM, has not resulted in a substantial improvement in the average survival of GBM patients. That new treatments are needed is an understatement.

Also in 1912, the idea of viral oncolytic treatment was born when Nicola De Pace reported that a series of women with cervical cancer experienced remission after receiving Pasteur’s rabies vaccine.³³ In recent years, interest in viral oncolytic treatment for GBM has increased.³⁴ ZIKV has particular appeal as an oncolytic virus for GBM given its affinity for neural progenitor cells.³⁵

Chen et al.²⁷ and Zhu et al.²⁶ showed that ZIKV is cytotoxic toward patient-derived glioma stem cells. Here we show that ZIKV is cytotoxic toward commercially available GBM cell lines that consist of both glioma stem cells and differentiated glioma cells. Moreover, this cytotoxicity is dose dependent with increased apoptosis and decreased cell viability with increasing MOI (Figure 5).

Another important feature of an oncolytic virus is its tropism for the intended target cancer cell. The AXL receptor is the candidate entry receptor for ZIKV in neural progenitor cells, radial glial cells, astrocytes, endothelial cells, and microglia.^{8,35} We reasoned that AXL might also function as an entry receptor in GBM cells given their common lineage. In this study, we first showed that cells that express AXL are permissive to ZIKV infection while those that do not are resistant to infection (Figure 1).

We next showed that pretreatment with an AXL antibody blocked ZIKV entry (Figures 2A and 2B). We also showed that AXL kinase activity was needed for productive infection, not just cell entry. ZIKV infection was reduced by pretreatment with the AXL kinase inhibitor R428 in a dose-dependent manner (Figures 2C–2F). Infection was also reduced by treating the cells 5 h after ZIKV exposure (Figures 3A and 3B). This is consistent with AXL’s role in innate immunity. Activation of AXL signaling pathways by virus binding depresses the type I interferon response.³⁶ Inhibition of AXL kinase activity by pretreating with R428 rescues the type I interferon response to intracellular ZIKV RNA, thus blocking viral replication.¹⁴ Our finding of post-exposure prevention of ZIKV replication is novel.

We further confirmed AXL as the entry receptor using our CRISPR AXL knockout cell lines: AXL knockouts were resistant to ZIKV infection whereas their parental cell lines were permissive (Figure 4). Adding AXL expression to a normally non-expressing cell line (MDA-468) or restoring AXL expression in an AXL CRISPR knockout cell line (U-251^{KO}) renders the cells permissive to ZIKV entry (Figure 6).

While our data are compelling, it remains unclear whether AXL is the sole entry receptor for ZIKV. Other investigators found that AXL was dispensable for ZIKV entry in induced pluripotent stem cell-derived cerebral organoids³⁷ in a TAM receptor knockout mouse model,²³ and following antibody blockade in human neural progenitor cells.¹⁴ Hastings et al., opined that human cells *in vivo* have alternative ZIKV entry receptors, and human cells *in vitro* do not faithfully capture this spectrum of entry receptors.²³ Meertens et al. suggest that ZIKV uses different receptors and signaling pathways based on cell type.¹⁴ To further understand the mechanisms of ZIKV cell entry, the experiments described in this report can be reproduced in patient-derived GBM primary cell lines.

Figure 4. CRISPR knockout of AXL prevents ZIKV infection

Confirmation of AXL knockout in (A) LN-229 and (B) U-251 MG cell lines using AXL CRISPR/Cas9 GFP Knockout plasmid. (C) LN-229 AXL^{KO} and parental cells were infected with ZIKV at MOI 1 and 10. The percentage of infected cells were quantified by flow cytometry at 48, 72, and 96 hpi. (D) LN-229 AXL^{KO} and parental cells were challenged with ZIKV at MOI 1 and 10. Total cellular RNA was extracted at 24 and 48 hpi. The relative levels of ZIKV NS3 RNA were determined by qRT-PCR. (E) U-251 MG AXL^{KO} and parental cells were exposed to ZIKV at MOI 1 and 10. After 72 hpi, the relative levels of ZIKV NS3 RNA were determined by qRT-PCR. (F) ZIKV titer (PFU/mL) comparison between parental and AXL knockout cell lines by plaque assay (n = 8 replicates) at 48 and 72 hpi. (G) Immunofluorescence staining for ZIKV in LN-229 AXL^{KO} and parental cells at 72 hpi at MOI 1 and 10. Scale bars, 100 μm. (H) Immunofluorescence staining of U-251 MG and U-251 MG AXL^{KO} 48 h after incubation with ZIKV. Scale bars, 500 μm. (I) Statistical analyses of IFA from (H) utilized two biological replicates performed in triplicate. A total of 30,000 cells were analyzed. Images were acquired through an Olympus IX83 microscope. ZIKV, green; DAPI, blue. In (D), (E), (F), and (I), data shown are means ± SD of averages of two independent experiments performed in triplicate. Significance was calculated using two-way ANOVA (n.s., not significant; ****p < 0.0001).

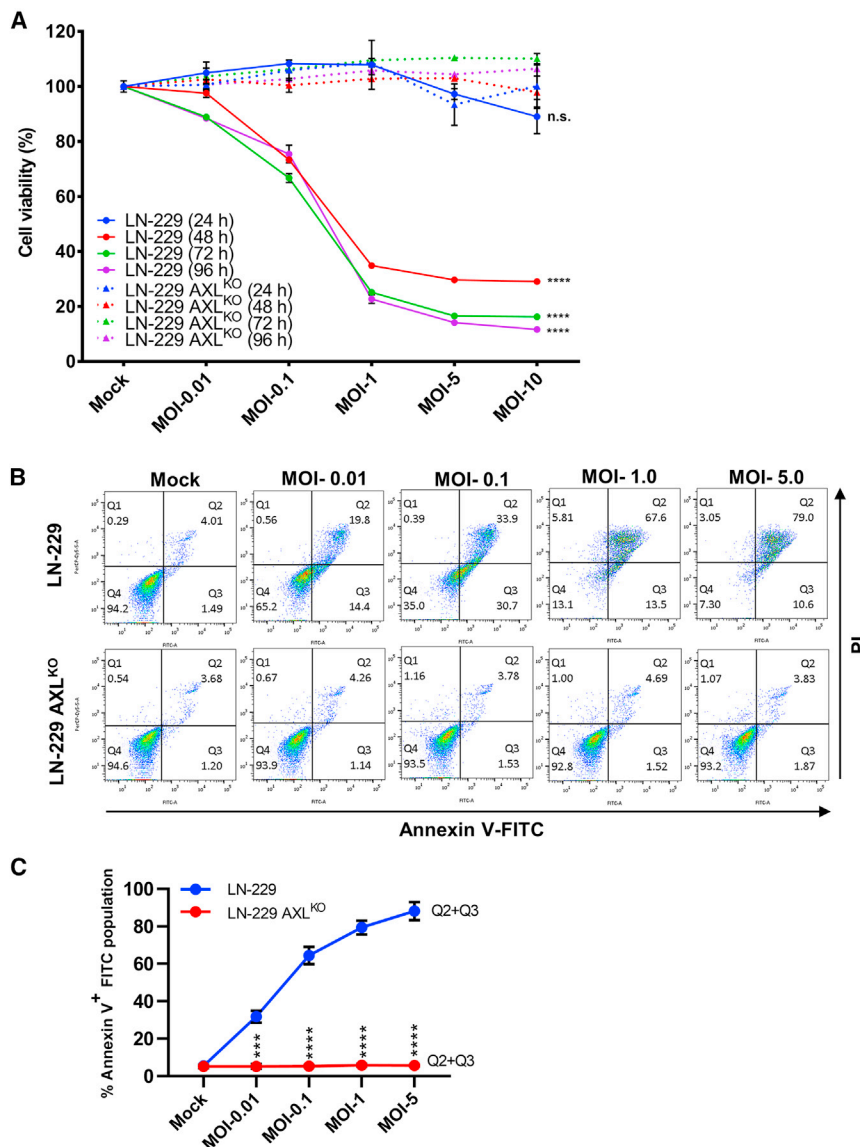


Figure 5. AXL^{KO} prevents cell death in glioblastoma cells *in vitro*

(A) LN-229 AXL^{KO} and parental cells were challenged with ZIKV at increasing MOI (0.01, 0.1, 1, 5, and 10) for 24, 48, 72, and 96 h. Cell viability was determined using WST-1 assay. (B) Flow-cytometry gating and acquired events in LN-229 AXL^{KO} and parental cells stained for propidium iodide (PI) and Annexin V at 72 hpi (n = 3 replicates per cell line). (C) Flow-cytometry staining analysis of PI and Annexin V. In (A) and (C), data shown are means ± SD of averages of three biological replicates, each biological replicate (n = 4) repeats. Significance was calculated using two-way ANOVA (n.s., not significant; ***p < 0.001, ****p < 0.0001).

LT07-710), before use in the described experiments. Cell lines were maintained in Dulbecco's modified Eagle's medium containing 10% fetal bovine serum (FBS) and 1% penicillin/streptomycin. All cell lines were incubated at 37°C in a humidified incubator supplemented with 5% CO₂.

Generation of AXL knockout (AXL^{KO}) cell lines

LN-229 and U-251 MG cells were electroporated with the AXL CRISPR/Cas9 GFP Knockout Plasmid (Santa Cruz Biotechnology, SC-400393) encoding the codon optimized Cas9 nuclease and three AXL-specific guide RNAs using the Neon Transfection kit (Thermo Fisher, MPK10096). Transfected cells were incubated for 48 h and GFP-expressing cells were sorted by fluorescence-activated cell sorting (BD FACSaria III Cell Sorter) into a 96-well plate. Single GFP-expressing cells were cultured and expanded for confirmation of AXL knockout using anti-AXL antibody. LN-229 AXL^{KO} and U-251 MG AXL^{KO} cells were maintained in standard culture conditions.

Generation of MDA-468::AXL and U-251 MG AXL^{KO}::AXL stable cell lines

The AXL lentivirus (pLenti-GIII-CMV-GFP-2A-Puro:AXL) was purchased from Applied Biological Materials (Richmond, BC, Canada, LVP086250). In brief, MDA-468 and U-251 MG AXL^{KO} cells were plated in 6-well plates and infected with the AXL lentivirus in the presence of 8 µg/mL polybrene at MOI of 1 for 3 days. After 3 days, successfully transduced cells were selected with puromycin (0.5 µg/mL used for MDA-468 and 3 µg/mL used for U-251 MG AXL^{KO}) for 5 days. After puromycin selection, these stably transduced cell lines were confirmed by immunoblot using AXL antibody.

Given its tropism for GBM cells through AXL, the overexpression of AXL in GBM,²⁴ and the cytotoxicity resulting from productive infection, we conclude that ZIKV is a candidate oncolytic virus for GBM.

MATERIALS AND METHODS

Cells and culture conditions

Human glioblastoma cell lines (LN-229, A-172, U-87 MG), human breast cancer cell line (MDA-468), and Vero cells (African green monkey kidney epithelial cells) were obtained from American Type Culture Collection (ATCC, Manassas, VA). The human glioblastoma cell line U-251 MG was obtained from Sigma-Aldrich (St Louis, MO). After thawing, cell lines were cultured under standard conditions for up to 2 weeks (2–3 passages) and tested routinely for mycoplasma contamination by using MycoAlert (Lonza,

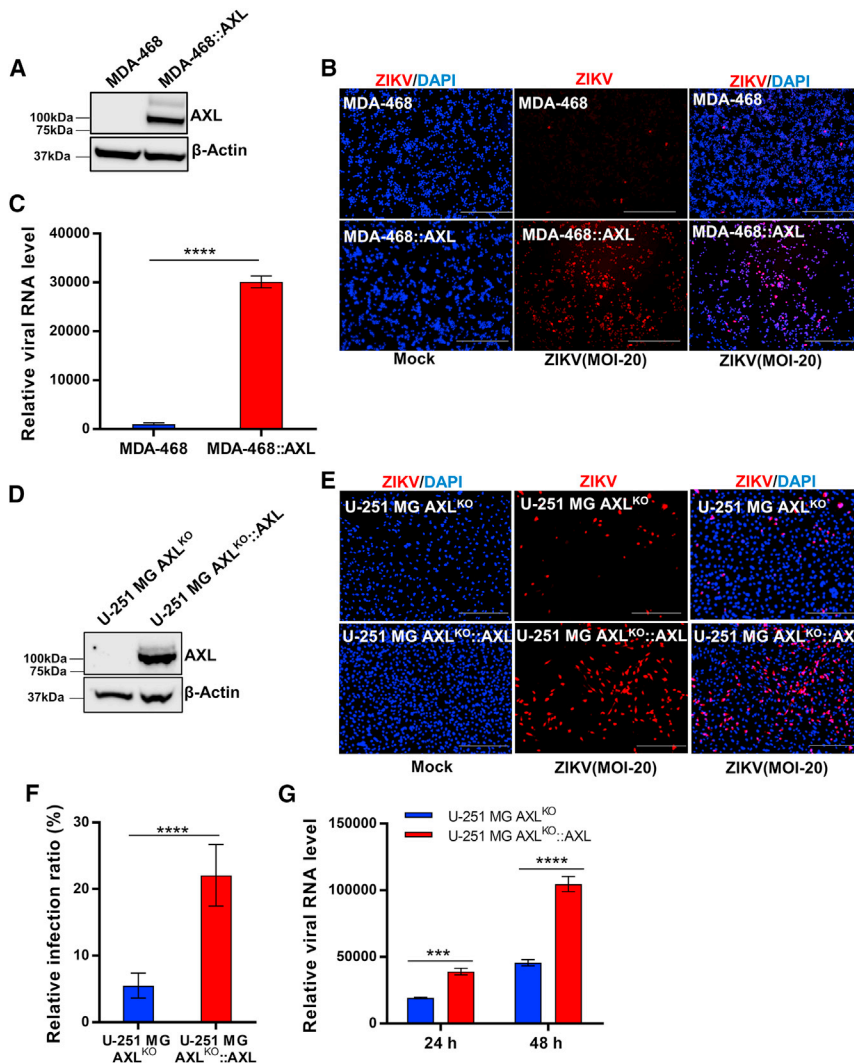


Figure 6. Stable AXL expression restores ZIKV entry

(A and D) Confirmation of AXL expression in MDA-468::AXL (A) and U-251 MG AXL^{KO}::AXL (D) cell lines by immunoblot. (B) Immunofluorescence staining shows ZIKV infection of MDA-468::AXL but not MDA-468. Scale bars, 500 μ m. (C) Relative expression of ZIKV NS3 RNA was quantified by qRT-PCR in MDA-468 and MDA-468::AXL cells at 5 days post infection and MOI of 20. (E) Immunofluorescence staining shows dramatic increase in ZIKV infection of U-251 MG AXL^{KO}::AXL cells compared with U-251 MG AXL^{KO} cells at 48 hpi. Scale bars, 500 μ m. (F) Statistical analyses of IFA were done from three biological replicates, a total of 36,000 analyzed cells. (G) Relative expression of ZIKV NS3 RNA was quantified by qRT-PCR in U-251 MG AXL^{KO} and U-251 MG AXL^{KO}::AXL cell lines at 24 and 48 hpi at MOI of 20. ZIKV, red; DAPI, blue. In (C), (F), and (G), data shown are means \pm SD from three independent experiments. Significance was calculated using a t test (***p < 0.001, ****p < 0.0001).

cells were washed once with PBS, and serial dilutions of ZIKV were made and then added to the cells for 2 h at 37°C to initiate binding. After 2 h, 2 mL of an OptiMEM GlutaMAX medium (Thermo Fisher) with 2% FBS and 1% methylcellulose (Sigma, M0512 4000 cps) overlay was added to the wells and incubated at 37°C for 5 days. For plaque counting and MOI calculation, the cells were fixed with 4% formaldehyde and stained with 0.8% crystal violet in 50% ethanol.

ZIKV titer in the supernatants of infected cell lines

LN-229, U-251 MG, A-172, U-87 MG, MDA-468, LN-229 AXL^{KO}, and U-251 MG AXL^{KO}

cell lines were infected with ZIKV (MOI 1), and ZIKV progeny titers were measured in the cell supernatants by plaque assay at 48 and 72 hpi.

Western blotting for AXL expression

Cells were collected and lysed in RIPA buffer with complete protease inhibitor cocktail (Roche). Lysates were resolved by 4%–12% SDS-PAGE and electrotransferred to nitrocellulose iBlot 2 Transfer Stacks (Life Technologies, IB23002). Membranes were blocked with 5% nonfat dried milk in 1 \times Tris-buffered saline and incubated overnight at 4°C with anti-AXL primary antibody (1:1,000 dilution; R&D Systems, AF154) or β -actin antibody (Sigma, A2066), and subsequently incubated for 1 h at room temperature with horseradish peroxidase-coupled secondary antibody. All membranes were scanned using the Odyssey infrared imaging system (LI-COR Biosciences) in conjunction with the Clarity Western ECL Substrate (Bio-Rad).

ZIKV propagation

ZIKV MR-766 strain (ATCC, VR-84) was propagated in Vero cells infected at an MOI of 0.01. In brief, diluted virus in Eagle's minimum essential medium (EMEM) without FBS was added to Vero cells and incubated/rocked for 2 h at 37°C in a humidified incubator. After incubation, EMEM with 2% FBS was added to the cells and incubated at 37°C in a humidified incubator with 5% CO₂. Supernatants were collected at 96 hpi, clarified by centrifugation at 500 \times g for 20 min, and kept at -80°C. For mock infections, supernatant was collected from uninfected Vero cells and prepared by the same protocol used to make viral stock. Passage history of the virus according to ATCC submission laboratories was: serial intracerebral passage in adult Swiss mice (146), suckling mice (1), ATCC: suckling mice (1).

ZIKV plaque assay

Viral titer (PFU/mL) was calculated by the plaque-forming assay using Vero cells. The Vero cells (5 \times 10⁵) were seeded in a 6-well plate and incubated at 37°C for 24 h before infection. The next day, Vero

Flow-cytometry analysis

Flow cytometry was used to determine the percentage of cells infected. For this analysis, cells were detached with trypsin-EDTA at indicated time points to remove cell surface bound viral particles and then washed with stain buffer (BD Biosciences, 554657). Cells were first stained with viability dye, eFluor 780 (Thermo Fisher, 65-0865-14) for 20 min at 4°C and then fixed with fixation solution (BD Biosciences, 51-2090KZ) for 20 min at 4°C. Intracellular viral antigens were stained under permeabilized condition (BD Biosciences, 554714) with primary flavivirus envelope protein monoclonal antibody 4G2 (Millipore, MAB10216) followed by a secondary staining with a phycoerythrin-conjugated goat anti-mouse IgG antibody (Jackson ImmunoResearch) in 1 × buffer. Acquisition was performed on an LSR Fortessa HTS flow cytometer with FACSDiva software (BD Biosciences), and data were analyzed using FlowJo v.10 software.

Viral RNA quantification

For viral RNA quantification, parental and AXL^{KO} cells were infected for the indicated lengths of time with ZIKV at MOI 1 or MOI 10 PFU/cell. Total RNA was extracted from infected cells, using the RNeasy Mini Kit (Qiagen), and the concentration was quantified by Nanodrop. Isolated RNAs (1 µg total RNA) were then digested with 1 unit of DNase I (NEB) at 37°C for 25 min to remove genomic DNA contamination before being processed for reverse transcription. qRT-PCR was performed using an iTaq Universal SYBR Green One-Step Kit (Bio-Rad, 1725151) according to the manufacturer's instructions on a Roche LightCycler 480 instrument. The primers for viral RNA quantification targeted the nonstructural protein NS3 (forward primer 5'-CCA ACA AAC CTG GAG ATG AGT A-3'; reverse primer 5'-GAG GCC ATC TTG GAG GTA AAT-3'). The control primers were GAPDH (forward primer 5'-GGA TTT GGT CGT ATT GGG-3'; reverse primer 5'-GGA AGA TGG TGA TGG GAT T-3'). Relative expression quantification was performed based on the comparative CT method ($2^{-\Delta\Delta Ct}$) using GAPDH as endogenous reference control.

Immunofluorescence staining

Productive ZIKV infection was qualitatively analyzed by IFA. Cells (2×10^5) were infected at MOI 1, 10, or 20 PFU/cell with ZIKV and cultured on Lab-Tek II 4-well chamber slides (Fisher Scientific) at indicated time points. Cells were washed with 1 × PBS and fixed with 4% paraformaldehyde for 15 min, then permeabilized with permeabilization buffer (BD Biosciences) for 30 min at room temperature. Cells were blocked with 10% normal goat serum (Cell Signaling Technology) for 1 h and then incubated with flavivirus envelope protein monoclonal antibody 4G2 (1:500; Millipore, MAB10216) for 2 h at room temperature. After incubation, cells were washed three times with PBS and incubated with Alexa Fluor 488-labeled anti-mouse antibody (Thermo Fisher, A11029) for 1 h at room temperature. Cells were then washed and mounted with Fluoroshield mounting medium containing 4',6-diamidino-2-phenylindole (DAPI; Abcam, ab104139) for nuclei staining. All images were acquired by a fluorescence microscope (Olympus IX83).

Antibody blockade and R428 inhibition of the AXL receptor

For antibody blockade, cells were treated with 10 µg of AXL antibody (R&D Systems, AF154) or goat IgG control (R&D Systems, AB108C) for 90 min before infection. Blocked cells were then infected at MOI of 10 PFU/cell with ZIKV for 90 min followed by medium change. Cells were cultured for 48 h before staining with flavivirus envelope 4G2 antibody for flow cytometry. In addition, a dose-response neutralization assay for the AXL antibody was used to calculate IC₅₀ values. In brief, increasing concentrations of AXL antibodies (1, 3, 5, 7, 10, and 12 µg/mL) were added to the cells for 90 min before subsequent ZIKV infection at MOI of 10 PFU/cell. Percentage of ZIKV-infected cells was determined by flow cytometry at 48 hpi. Dose-response curves were generated and IC₅₀ values calculated for LN229, U-87 MG, and A-172 cell lines.

For determination of whether R428 treatment prevents ZIKV entry, LN-229, U-87 MG, and A-172 cells were pretreated with 0.3 µM or 1 µM R428 (ApexBio; A8329) or vehicle (<0.1% dimethyl sulfoxide [DMSO]) for 90 min before infection. Treated cells were then exposed to ZIKV at MOI of 10 for 90 min, then the medium was changed. The percentage of cells infected with ZIKV at 32 hpi was quantified with flow cytometry. To determine whether R428 treatment prevents ZIKV replication, we first exposed LN-229 and U-87 MG cells to ZIKV at MOI of 1 PFU/cell for 90 min. The cells were washed and incubated for 5 h and then treated with 0.3 µM or 1 µM R428. The percentage of infected cells was determined by flow cytometry after culture for 24 h.

The effect of R428 alone on cell viability was evaluated by treating LN-229, U-87 MG, and A-172 cells with vehicle or R428 at 0.1, 0.3, and 1 µM. After 32 h, viability was determined using the WST-1 (Roche) assay.

ZIKV infection of AXL^{KO} cell lines

LN-229 and LN-229 AXL^{KO} cells were exposed to ZIKV at MOI 1 or MOI 10 PFU/cell for 90 min followed by medium change, then incubated at indicated time points, after which the percentage of infected cells was determined by flow cytometry. Parental and LN-229 AXL^{KO} and U-251 MG AXL^{KO} cells were infected with ZIKV at MOI 1 or MOI 10 PFU/cell and incubated at indicated time points, and intracellular viral RNA was evaluated by qRT-PCR.

ZIKV infection of MDA-468::AXL and U-251 MG AXL^{KO}::AXL stable cell lines

Parental and MDA-468::AXL and U-251 MG AXL^{KO}::AXL cell lines were exposed to ZIKV at MOI of 20 PFU/cell for 90 min followed by medium change and incubated at indicated time points. The percentage of infection was calculated from immunofluorescence staining, and intracellular viral RNA was evaluated by qRT-PCR.

WST-1 assay

Cell viability after ZIKV infection was assessed using the WST-1 (Roche) assay according to the manufacturer's instructions. LN-229 and LN-229 AXL^{KO} were exposed to ZIKV at MOI 0.01, 0.1, 1, 5,

and 10 PFU/cell. After 90 min the cells were washed, then cultured at 37°C in 96-well plates at a density of 50,000 cells per well in 100 µL of medium for 24, 48, 72, and 96 h. At the indicated time points, 10 µL of WST-1 reagent was added to the wells and the plate was incubated at 37°C and 5% CO₂ for 1 h. The absorbance values were then measured at 450 nm against a background using a microplate reader (BioTek).

Annexin V assay

LN-229 and LN-229 AXL^{KO} cells (1×10^5) were infected with ZIKV at MOI 0.01, 0.1, 1, and 5 PFU/cell. At 72 hpi the cells were stained for Annexin V (FITC Annexin V Apoptosis Detection Kit II, BD Biosciences) and propidium iodide following the manufacturer's protocol. Flow-cytometry analysis was immediately performed on a BD LSR Fortessa HTS flow cytometer collecting 10,000 events per run. Data analysis was then carried out using FlowJo software.

Statistical analyses

All statistical analyses were performed using Prism 7 software (GraphPad). The number of replicates included in each experiment is specified in each figure legend. Data are represented graphically as mean \pm standard deviation (SD). One-way ANOVA, two-way ANOVA, and t test were used to determine the significance of variation between groups. p-value thresholds were as follows: n.s., not significant; **p < 0.01, ***p < 0.001, ****p < 0.0001.

SUPPLEMENTAL INFORMATION

Supplemental information can be found online at <https://doi.org/10.1016/j.omto.2021.11.001>.

ACKNOWLEDGMENTS

This study was supported by Intramural Oncology Research Award, Advocate Aurora Research Institute, Aurora Health Care Foundation, Vince Lombardi Cancer Foundation, E. C. Styberg Foundation, Wisconsin, United States (grant 570-5039 to P.A.). We are very grateful for Dr. Guillaume Curaudeau for designing the graphical abstract for this study. We thank Dr. Maharaj Singh for helping with statistical analysis, Dmitry Bosenko, Deborah Donohoe, Kate Dennert, Logan Friedrich, and Aspen Duffin for technical assistance in the lab, and Dr. John Richards, Dr. Santhi Konduri, Dr. Farhan Rizvi, and Dr. Yin Jun for helpful discussions.

AUTHOR CONTRIBUTIONS

S.D.Z.: methodology, data curation, formal analysis, writing – review & editing. B.H.A.: data curation, writing – review & editing. D.A.R.: formal analysis, writing – review & editing. C.M.W.: data curation, writing – review & editing. A.B.K.: resources, writing – review & editing. R.A.R.: conceptualization, resources, visualization, supervision, writing – review & editing. P.A.: conceptualization, funding acquisition, methodology, data curation, formal analysis, investigation, supervision, resources, visualization, writing – original draft.

DECLARATION OF INTERESTS

The authors declare no competing interests.

REFERENCES

- Davis, M.E. (2016). Glioblastoma: overview of disease and treatment. *Clin. J. Oncol. Nurs.* 20, S2–S8. <https://doi.org/10.1188/16.Cjon.S1.2-8>.
- Stupp, R., Mason, W.P., van den Bent, M.J., Weller, M., Fisher, B., Taphoorn, M.J., Belanger, K., Brandes, A.A., Marosi, C., Bogdahn, U., et al. (2005). Radiotherapy plus concomitant and adjuvant temozolomide for glioblastoma. *N. Engl. J. Med.* 352, 987–996. <https://doi.org/10.1056/NEJMoa043330>.
- Kaufman, H.L., Kohlhapp, F.J., and Zloza, A. (2015). Oncolytic viruses: a new class of immunotherapy drugs. *Nat. Rev. Drug Discov.* 14, 642–662. <https://doi.org/10.1038/nrd4663>.
- Peruzzi, P., and Chiocca, E.A. (2018). Viruses in cancer therapy- from benchwarmers to quarterbacks. *Nat. Rev. Clin. Oncol.* 15, 657–658. <https://doi.org/10.1038/s41571-018-0077-0>.
- Garcez, P.P., Loiola, E.C., Madeiro da Costa, R., Higa, L.M., Trindade, P., Delvecchio, R., Nascimento, J.M., Brindeiro, R., Tanuri, A., and Rehen, S.K. (2016). Zika virus impairs growth in human neurospheres and brain organoids. *Science* 352, 816–818. <https://doi.org/10.1126/science.aaf6116>.
- Ming, G.L., Tang, H., and Song, H. (2016). Advances in Zika virus research: stem cell models, challenges, and opportunities. *Cell Stem Cell* 19, 690–702. <https://doi.org/10.1016/j.stem.2016.11.014>.
- Mlakar, J., Korva, M., Tul, N., Popovic, M., Poljsak-Prijatelj, M., Mraz, J., Kolenc, M., Resman Rus, K., Vesnaver Vipotnik, T., Fabjan Vodusek, V., et al. (2016). Zika virus associated with microcephaly. *N. Engl. J. Med.* 374, 951–958. <https://doi.org/10.1056/NEJMoa1600651>.
- Nowakowski, T.J., Pollen, A.A., Di Lullo, E., Sandoval-Espinosa, C., Bershteyn, M., and Kriegstein, A.R. (2016). Expression analysis highlights AXL as a candidate Zika virus entry receptor in neural stem cells. *Cell Stem Cell* 18, 591–596. <https://doi.org/10.1016/j.stem.2016.03.012>.
- Retallack, H., Di Lullo, E., Arias, C., Knopp, K.A., Laurie, M.T., Sandoval-Espinosa, C., Mancia Leon, W.R., Krencik, R., Ullian, E.M., Spatazza, J., et al. (2016). Zika virus cell tropism in the developing human brain and inhibition by azithromycin. *Proc. Natl. Acad. Sci. U S A* 113, 14408–14413. <https://doi.org/10.1073/pnas.1618029113>.
- Li, H., Saucedo-Cuevas, L., Regla-Nava, J.A., Chai, G., Sheets, N., Tang, W., Terskikh, A.V., Shresta, S., and Gleeson, J.G. (2016). Zika virus infects neural progenitors in the adult mouse brain and alters proliferation. *Cell Stem Cell* 19, 593–598. <https://doi.org/10.1016/j.stem.2016.08.005>.
- Gay, C.M., Balaji, K., and Byers, L.A. (2017). Giving AXL the axe: targeting AXL in human malignancy. *Br. J. Cancer* 116, 415–423. <https://doi.org/10.1038/bjc.2016.428>.
- Axelrod, H., and Pienta, K.J. (2014). Axl as a mediator of cellular growth and survival. *Oncotarget* 5, 8818–8852. <https://doi.org/10.18632/oncotarget.2422>.
- Wu, X., Liu, X., Koul, S., Lee, C.Y., Zhang, Z., and Halmos, B. (2014). AXL kinase as a novel target for cancer therapy. *Oncotarget* 5, 9546–9563. <https://doi.org/10.18632/oncotarget.2542>.
- Meertens, L., Labeau, A., Dejarnac, O., Cipriani, S., Sinigaglia, L., Bonnet-Madin, L., Le Charpentier, T., Hafirassou, M.L., Zamborlini, A., Cao-Lormeau, V.M., et al. (2017). Axl mediates ZIKA virus entry in human glial cells and modulates innate immune responses. *Cell Rep.* 18, 324–333. <https://doi.org/10.1016/j.celrep.2016.12.045>.
- Chen, J., Yang, Y.F., Yang, Y., Zou, P., Chen, J., He, Y., Shui, S.L., Cui, Y.R., Bai, R., Liang, Y.J., et al. (2018). AXL promotes Zika virus infection in astrocytes by antagonizing type I interferon signalling. *Nat. Microbiol.* 3, 302–309. <https://doi.org/10.1038/s41564-017-0092-4>.
- Richard, A.S., Shim, B.S., Kwon, Y.C., Zhang, R., Otsuka, Y., Schmitt, K., Berri, F., Diamond, M.S., and Choe, H. (2017). AXL-dependent infection of human fetal endothelial cells distinguishes Zika virus from other pathogenic flaviviruses. *Proc. Natl. Acad. Sci. U S A* 114, 2024–2029. <https://doi.org/10.1073/pnas.1620558114>.
- Liu, S., DeLalio, L.J., Isakson, B.E., and Wang, T.T. (2016). AXL-mediated productive infection of human endothelial cells by Zika virus. *Circ. Res.* 119, 1183–1189. <https://doi.org/10.1161/circresaha.116.309866>.
- Hamel, R., Dejarnac, O., Wicht, S., Ekchariyawat, P., Neyret, A., Luplertlop, N., Perera-Lecoin, M., Surasombattana, P., Talignani, L., Thomas, F., et al. (2015). Biology of Zika virus infection in human skin cells. *J. Virol.* 89, 8880–8896. <https://doi.org/10.1128/jvi.00354-15>.

19. Strange, D.P., Jiyarom, B., Pourhabibi Zarandi, N., Xie, X., Baker, C., Sadri-Ardekani, H., Shi, P.Y., and Verma, S. (2019). Axl promotes Zika virus entry and modulates the antiviral state of human sertoli cells. *mBio* 10, e01372. <https://doi.org/10.1128/mBio.01372-19>.
20. Mazar, J., Li, Y., Rosado, A., Phelan, P., Kedarinath, K., Parks, G.D., Alexander, K.A., and Westmoreland, T.J. (2018). Zika virus as an oncolytic treatment of human neuroblastoma cells requires CD24. *PLoS One* 13, e0200358. <https://doi.org/10.1371/journal.pone.0200358>.
21. Tan, C.W., Huan Hor, C.H., Kwek, S.S., Tee, H.K., Sam, I.C., Goh, E.L.K., Ooi, E.E., Chan, Y.F., and Wang, L.F. (2019). Cell surface alpha2,3-linked sialic acid facilitates Zika virus internalization. *Emerg. Microbes Infect.* 8, 426–437. <https://doi.org/10.1080/22221751.2019.1590130>.
22. Srivastava, M., Zhang, Y., Chen, J., Sirohi, D., Miller, A., Zhang, Y., Chen, Z., Lu, H., Xu, J., Kuhn, R.J., et al. (2020). Chemical proteomics tracks virus entry and uncovers NCAM1 as Zika virus receptor. *Nat. Commun.* 11, 3896. <https://doi.org/10.1038/s41467-020-17638-y>.
23. Hastings, A.K., Yockey, L.J., Jagger, B.W., Hwang, J., Uraki, R., Gaitsch, H.F., Parnell, L.A., Cao, B., Mysorekar, I.U., Rothlin, C.V., et al. (2017). TAM receptors are not required for Zika virus infection in mice. *Cell Rep.* 19, 558–568. <https://doi.org/10.1016/j.celrep.2017.03.058>.
24. Wang, Z.Y., Wang, Z., Zhen, Z.D., Feng, K.H., Guo, J., Gao, N., Fan, D.Y., Han, D.S., Wang, P.G., and An, J. (2017). Axl is not an indispensable factor for Zika virus infection in mice. *J. Gen. Virol.* 98, 2061–2068. <https://doi.org/10.1099/jgv.0.000886>.
25. Hutterer, M., Knyazev, P., Abate, A., Reschke, M., Maier, H., Stefanova, N., Knyazeva, T., Barbieri, V., Reindl, M., Muigg, A., et al. (2008). Axl and growth arrest-specific gene 6 are frequently overexpressed in human gliomas and predict poor prognosis in patients with glioblastoma multiforme. *Clin. Cancer Res.* 14, 130–138. <https://doi.org/10.1158/1078-0432.Ccr-07-0862>.
26. Zhu, Z., Gorman, M.J., McKenzie, L.D., Chai, J.N., Hubert, C.G., Prager, B.C., Fernandez, E., Richner, J.M., Zhang, R., Shan, C., et al. (2017). Zika virus has oncolytic activity against glioblastoma stem cells. *J. Exp. Med.* 214, 2843–2857. <https://doi.org/10.1084/jem.20171093>.
27. Chen, Q., Wu, J., Ye, Q., Ma, F., Zhu, Q., Wu, Y., Shan, C., Xie, X., Li, D., Zhan, X., et al. (2018). Treatment of human glioblastoma with a live attenuated Zika virus vaccine candidate. *mBio* 9. <https://doi.org/10.1128/mBio.01683-18>.
28. Lubin, J.A., Zhang, R.R., and Kuo, J.S. (2018). Zika virus has oncolytic activity against glioblastoma stem cells. *Neurosurgery* 82, E113–E114. <https://doi.org/10.1093/neuros/nyy047>.
29. Kaid, C., Goulart, E., Caires-Junior, L.C., Araujo, B.H.S., Soares-Schanoski, A., Bueno, H.M.S., Telles-Silva, K.A., Astray, R.M., Assoni, A.F., Junior, A.F.R., et al. (2018). Zika virus selectively kills aggressive human embryonal CNS tumor cells in vitro and in vivo. *Cancer Res.* 78, 3363–3374. <https://doi.org/10.1158/0008-5472.Can-17-3201>.
30. Zhu, Z., Mesci, P., Bernatchez, J.A., Gimple, R.C., Wang, X., Schafer, S.T., Wettersten, H.I., Beck, S., Clark, A.E., Wu, Q., et al. (2020). Zika virus targets glioblastoma stem cells through a SOX2-integrin $\alpha_v\beta_5$ axis. *Cell Stem Cell* 26, 187–204.e10. <https://doi.org/10.1016/j.stem.2019.11.016>.
31. Su, K.Y., and Balasubramanian, V. (2019). Zika virus as oncolytic therapy for brain cancer: myth or reality? *Front Microbiol.* 10, 2715. <https://doi.org/10.3389/fmicb.2019.02715>.
32. Tooth, H.H. (1912). Some observations on the growth and survival-period of intracranial tumours, based on the records of 500 cases, with special reference to the pathology of the gliomata. *Brain* 35, 61–108.
33. De Pace, N. (1912). Sulla scomparsa di un enorme cancro vegetante del collo dell'utero senza cura chirurgica. *Ginecologia* 9, 82–89.
34. Foreman, P.M., Friedman, G.K., Cassady, K.A., and Markert, J.M. (2017). Oncolytic virotherapy for the treatment of malignant glioma. *Neurotherapeutics* 14, 333–344. <https://doi.org/10.1007/s13311-017-0516-0>.
35. Tang, H., Hammack, C., Ogden, S.C., Wen, Z., Qian, X., Li, Y., Yao, B., Shin, J., Zhang, F., Lee, E.M., et al. (2016). Zika virus infects human cortical neural progenitors and attenuates their growth. *Cell Stem Cell* 18, 587–590. <https://doi.org/10.1016/j.stem.2016.02.016>.
36. Bhattacharyya, S., Zagórska, A., Lew, E.D., Shrestha, B., Rothlin, C.V., Naughton, J., Diamond, M.S., Lemke, G., and Young, J.A. (2013). Enveloped viruses disable innate immune responses in dendritic cells by direct activation of TAM receptors. *Cell Host Microbe* 14, 136–147. <https://doi.org/10.1016/j.chom.2013.07.005>.
37. Wells, M.F., Salick, M.R., Wiskow, O., Ho, D.J., Worringer, K.A., Ihry, R.J., Kommineni, S., Bilican, B., Klim, J.R., Hill, E.J., et al. (2016). Genetic ablation of AXL does not protect human neural progenitor cells and cerebral organoids from Zika virus infection. *Cell Stem Cell* 19, 703–708. <https://doi.org/10.1016/j.stem.2016.11.011>.